Article

Embeddings of Graphs. Tessellate and Decussate Structures.

Michael O'Keeffe and Michael Matthew John Treacy *

Posted Date: 4 October 2023

doi: 10.20944/preprints202310.0188.v1

Keywords: Graph; topology; ambient isotopy; periodic net; tessellate; decussate

Article

Embeddings of Graphs. Tessellate and Decussate Structures

Michael O'Keeffe [1] and Michael M. J. Treacy [2,*]

[1] School of Molecular Sciences, Arizona State University, Tempe, Arizona 85287, USA; mokeeffe@asu.edu
[2] Department of Physics, Arizona State University, Tempe, Arizona 85287, USA.
* Correspondence: treacy@asu.edu

Abstract: We address the problem of finding a unique graph embedding that best describes a graph's "topology". This issue is of particular interest in the chemistry of materials. Graphs that admit a tiling in 3-dimensional Euclidean space are termed *tessellate*, those that do not *decussate*. We give examples of decussate and tessellate graphs that are finite and 3-periodic. We conjecture that a graph has at most one tessellate embedding. We give reasons for considering this the default "topology" of periodic graphs.

Keywords: Graph; topology; ambient isotopy; periodic net; tessellate; decussate

1. Introduction

1.1. General

This article is a sequel to our earlier article, *The Symmetry and Topology of Finite and Periodic Graphs and Their Embeddings in Three-Dimensional Euclidean Space* [1]. In this article, which continues to have tutorial aspects, we address the question of whether there is a canonical ("best") embedding ("topology") of a graph in Euclidean space.

We remind the reader of the generally accepted meanings of *topology* and *graph*. From the Oxford Dictionary of Mathematics [2]:

Topology: The area of mathematics concerned with the general properties of shapes and space, and in particular with the study of properties that are not changed by continuous distortions.

Graph: A number of vertices, some of which are joined by edges.

It is a common practice to analyze the structures of chemical compounds in terms of underlying graphs that describe the linking of components. This is commonly done by determining graph invariants such as coordination sequences and vertex symbols. Although not rigorously unique identifiers, in practice, these are reliable when used by programs like *ToposPro* [3]. For most 2- and 3-periodic graphs, the program *Systre* [4] definitively identifies the graph given crystallographic definitions of edges. Graphs are commonly identified by a 3-letter lower-case-bold symbol such as **dia** for the graph of the diamond structure. So far, so good; but the trouble comes when, as almost invariably, the result is reported as "a structure" having "the **dia** topology".

A graph can have many embeddings with different topologies. So, what is meant by "the **dia** topology"? The 3-letter lower-case-bold symbols originate in the Reticular Chemistry Structure Resource (RCSR) [5]. This is a collection of embedded graphs and includes such things as interwoven (interlinked) nets, knots, links, and alternative embeddings of a given graph – all with different *topologies*.

A problem is that the "diamond graph", for example, can have embeddings with different topologies (belonging to different *ambient isotopies*). One such alternative embedding in actual materials is known to RCSR as **dia-z**. If *ToposPro* or *Systre* analyze a structure based on that topology, the graph is again reported correctly as the **dia** graph, but its structure and that of diamond are not ambient isotopes – they have different topologies. Other examples of alternative embeddings of 3-periodic graphs were given in the earlier paper [1]. Here we attempt to clarify the ambiguity in nomenclature.

Preprints (www.preprints.org) | NOT PEER-REVIEWED | Posted: 4 October 2023 doi:10.20944/preprints202310.0188.v1

1.2. Terminology and Definitions

We are concerned with tilings that fill space with generalized polyhedral *cages*, which may have 2-coordinated vertices, but never 1-coordinated (*leaves*) or 0-coordinated vertices (isolated vertices). A face symbol $[M_m.N_n.\dots]$ indicates that the tile has m M-sided faces, n N-sided faces, etc. Tiles with 2-coordinated vertices are called *cages*. They are often extended polyhedra in which 2-coordinated vertices are inserted in some or all edges of the polyhedron. Figure 1 shows examples of cages that are of particular interest in what follows. An n-theta graph is a graph of just two vertices joined by n edges. The extended 4-theta graph is an important space-filling solid, as is the tile of the net, **bcu**, of the body-centered cubic lattice.

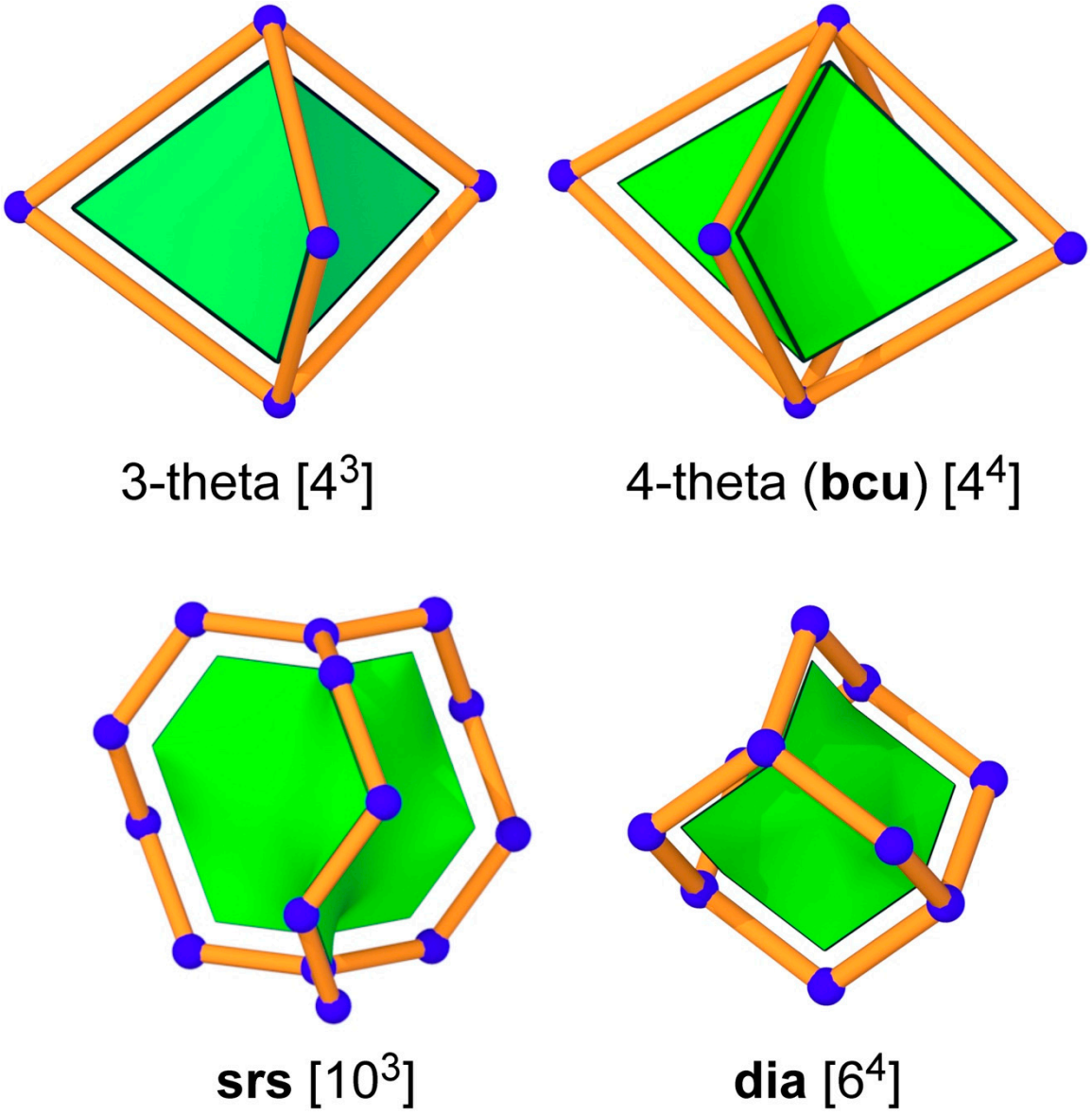

Figure 1. Examples of cages. All but the extended 3-theta (top left) are space-filling. The tile of the **dia** graph is an extended tetrahedron.

If a tiling has p kinds of symmetry-related vertices, q kinds of edges, r kinds of faces, and s kinds of tiles, the *transitivity* is expressed as $[p\ q\ r\ s]$. For a graph, we similarly express the number of kinds of vertices and edges by $[p\ q]$. Vertex-transitive structures are termed *isogonal*. Tilings with the full symmetry of the graph they carry are termed *proper tilings* [6].

All our structures are 3-dimensional and exist in Euclidean space. They may be 0-, 1-, 2-, or 3-periodic. Their symmetries are the point, rod, plane, layer, or space groups – best expressed in the

 doi:10.20944/preprints202310.0188.v1

Hermann-Mauguin (International) symbolism [1]. Structures whose graph admits a tiling are called *tessellate*, and those that do not are termed *decussate*; a word that comes from the Latin word for 10 (symbol X) and means having crossings (as in weaving). The vertices of graphs can be assigned *barycentric* coordinates in which the coordinates of a vertex are the mean of the coordinates of its neighbors. The graph is said to have *collisions* if two or more vertices have the same barycentric coordinates. An important result [4] is that for a periodic graph without collisions, the full symmetry of the graph is a crystallographic space group and *Systre* can always identify that "maximum symmetry" group. Graphs with collisions are of minor importance in the chemistry of materials; for examples see our earlier paper [1].

An adjacency matrix readily specifies a finite graph. However, showing that two graphs are the same requires identifying a vertex numbering that is the same in both matrices. Since there are $N!$ ways to number a graph with N vertices this becomes practically impossible for large N. This issue is at the heart of the so-called "graph isomorphism problem". For periodic graphs, the quotient graph can be given [4]. In this case, a unique vertex-numbering can be found for graphs in which all vertices have non-identical barycentric coordinates. Such graphs are termed "crystallographic" as their symmetries are crystallographic space groups. The program *Systre* [4] unambiguously determines the identity and symmetry of such graphs.

For a given straight-edge (*piecewise-linear*) graph embedding, we define *girth* as the ratio of the shortest distance between edges to the length of the longest edge. Girth is, in effect, a measure of the maximum stoutness of the sticks with which the edges of the structure can be built without any stick overlap. For many embeddings, sticks are slender (low girth). The larger-girth embeddings are particularly interesting to us as they represent structures that are easier to build as molecules. In finding possible embeddings of graphs for a given symmetry, we first identify edges between vertices i and j, x_i, y_i, z_i to x_j, y_j, z_j. We then search coordinate space for the *local* maximum girth by a gradient-descent method. Generally, to go from one maximum girth to another, some edges must cross, forcing the girth to pass through zero, transforming the structure to a topologically different embedding – to a different ambient isotopy. Occasionally, two or more local (ambient isotopic) maxima arise corresponding to the same topology but separated by "logjams"; that is, the girth must decrease momentarily to unjam the structure, thereby allowing the global maximum girth to be reached without any stick intersections. In crucial cases, we can visually inspect different embeddings to verify they are different topologies. We give examples below.

2. Embeddings of finite graphs

Finite graphs have long been classified as *planar* or *nonplanar*. A planar graph has a 2-dimensional embedding without intersecting edges. If a planar graph is 3-connected – meaning that at least 3 vertices and their incident edges must be deleted to separate the graph into disjoint components – the graph is then the graph of a polyhedron. A 2-dimensional embedding of the graph of a polyhedron is known as a *Schlegel diagram*. Note that the perimeter of the Schlegel diagram is a face of the polyhedron. Figure 2 shows two simple examples of Schlegel diagrams. These are clearly tessellate embeddings. In our earlier paper [1] we showed alternative embeddings of the cube graph. These all contained either links or knots as subgraphs, and those alternative embeddings are therefore decussate. This leads to the, perhaps "obvious", conclusion that the unique tessellate embedding of a polyhedron graph can be interpreted as the *canonical embedding*.

Preprints (www.preprints.org) | NOT PEER-REVIEWED | Posted: 4 October 2023 doi:10.20944/preprints202310.0188.v1

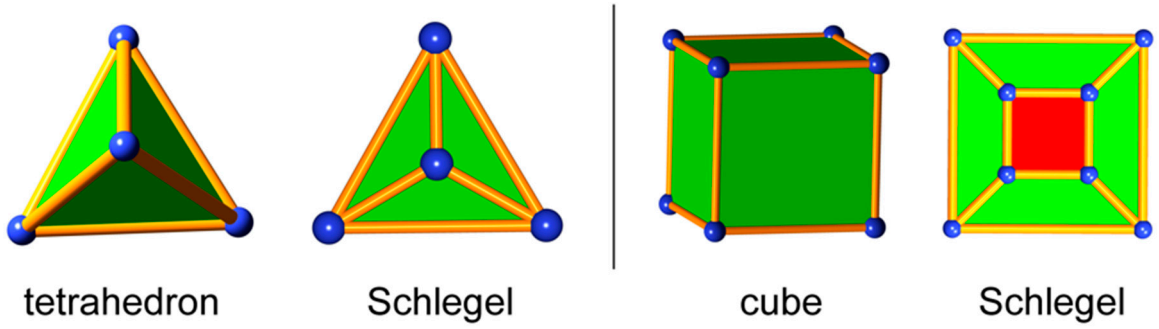

Figure 2. Examples of Schlegel diagrams for 3-dimensional polyhedra.

A well-established result is that every nonplanar graph contains, as a subgraph, either the complete graph on five vertices, K_5, or the complete bipartite graph on two sets of three vertices, $K_{3,3}$. It is instructive to further examine complete and bipartite graphs. For complete graphs, it was shown [7] that every embedding of K_6 in 3-dimensional Euclidean space contains two linked triangles, and every embedding of K_7 contains a knot. As noted earlier [1], K_n has an automorphism group that is the permutation group S_n of order $n!$. S_4 is isomorphic with the tetrahedral group, but no symmetry group in 3-D Euclidean space contains S_n for $n > 4$.

In Figure 3 we show embeddings of K_5, K_6, and K_7. For K_5 there is a tessellate embedding of 4 tetrahedra inside an envelope of a fifth tetrahedron. This is the Schlegel diagram of the 4-dimensional simplex and seems clearly to be the canonical embedding in 3-D; the symmetry is $\bar{4}3m$. For K_6 the situation is less clear. In one embedding shown, with symmetry $\bar{4}2m$, the transitivity is [2 4], and contains the predicted link of 2 triangles (light blue edges). However, we also show an embedding in symmetry 32, with transitivity [1 4], which is now "more tangled" as it also contains a trefoil knot (light blue edges). These two embeddings of the same graph are not ambient isotopic, and this leaves the question of a canonical embedding of "the topology" of the graph moot since neither is tessellate. An embedding is found for K_7 by adding an extra vertex to the 32 embedding of K_6, which includes the predicted knot. The transitivity of the embedding is now [2 5]. We remark that a graph of transitivity [1 1], and automorphism group of order 7! = 8040 has a "best" embedding in 3-D with symmetry of order 6 and transitivity [2 5], albeit still decussate.

Preprints (www.preprints.org) | NOT PEER-REVIEWED | Posted: 4 October 2023 doi:10.20944/preprints202310.0188.v1

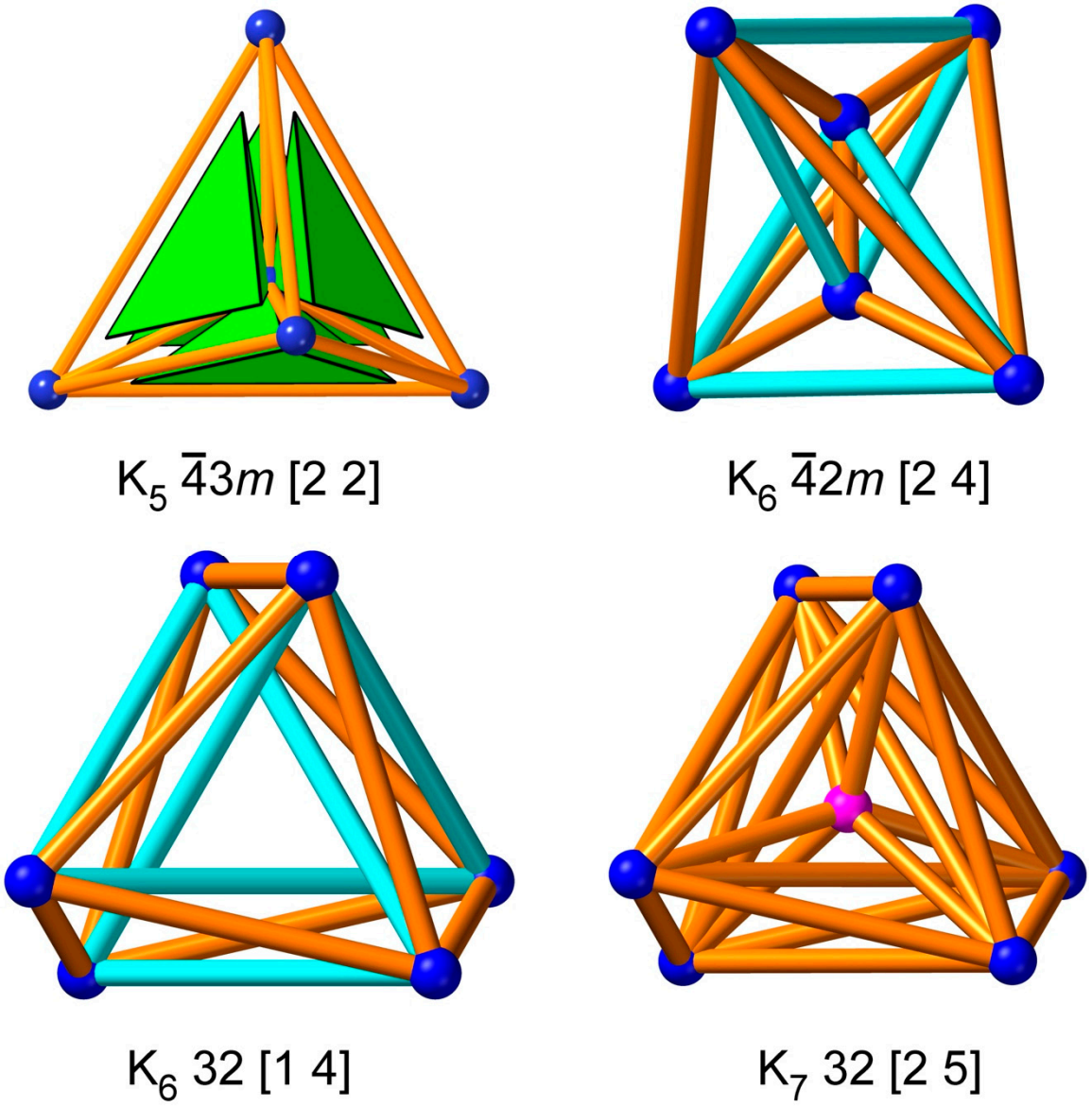

Figure 3. Embeddings of finite complete graphs. The embedding of K_5 is tessellate – four tetrahedra inside a larger tetrahedron, and the Schlegel diagram of the 4-dimensional simplex. For clarity, these are not depicted at maximum girth.

Turning to the bipartite graphs K_{nn}: One, K_{33}, is known as a "Möbius ladder graph" [8] and has been recognized in a chemical structure [9]. This embedding, with symmetry 32, and transitivity [1 3], is shown in Figure 4; this is clearly decussate as it contains a trefoil knot as a subgraph. We also show a second embedding with symmetry $\bar{6}m2$, transitivity [3 3]. This is now tessellate, the tiling consisting of two extended 3-theta cages inside an envelope that is also an extended 3-theta cage. The situation is similar for K_{44}. There is an isogonal decussate embedding with symmetry 422, transitivity [1 4] that contains the 8-crossing torus knot, 8_{19}. There is also an embedding with symmetry $4/mmm$, transitivity [3 3], that is tessellate with tiles that are extended 4-theta cages. Generalizing for K_{nn}, there are isogonal decussate embeddings with symmetry $n2$ (n odd) or $n22$ (n even) and a second tessellate embedding with symmetry $\overline{(2n)}m2$ (n odd) or n/mmm (n even). The tessellate embedding has n extended n-theta cages as tiles. Here, the question of the best or "canonical" embedding is a choice between an isogonal decussate embedding or a non-isogonal tessellate embedding.

Preprints (www.preprints.org) | NOT PEER-REVIEWED | Posted: 4 October 2023 doi:10.20944/preprints202310.0188.v1

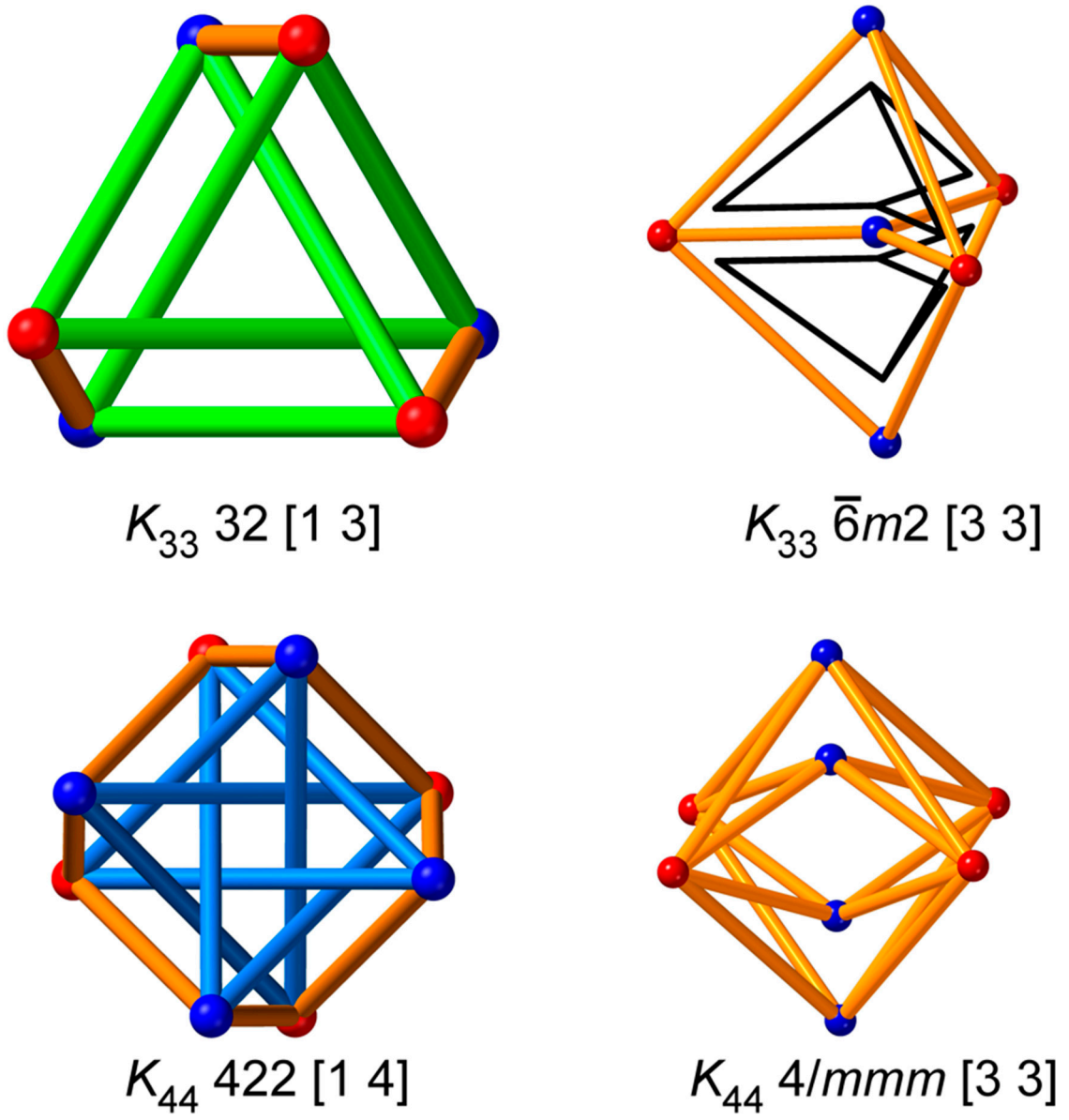

Figure 4. Embeddings of complete bipartite graphs. On the left is a decussate embedding, on the right a tessellate embedding. In the decussate embedding of K_{33} (top right) two extended 3-theta tiles (black lines) inside a larger extended 3-theta tile are indicated.

3. Embeddings of periodic graphs

We note first that 3-periodic graphs may be tessellate or decussate, or both, and that the tiles of a tiling may be polyhedra or cages, or both. We deal with simple periodic structures for which the intrinsic symmetry is a crystallographic space group; the so-called *crystallographic graphs* [1]. For such a structure, a maximum-symmetry tiling is a *proper tiling* [6]. There may be more than one proper tiling, but they all carry the same embedding of the net. There also may be possibilities for lower symmetry tilings of a net. In Figure 5, we show examples of lower-symmetry embeddings of **pcu**. Clearly, these carry the same embedding of the **pcu** graph. We conjecture that:

If a graph admits tilings, all tilings carry ambient isotopic embeddings of that graph.

We turn now to embeddings in general. Changing the unit cell parameters of an embedding of a periodic graph only affects the scale (uniform compression or expansion) or shear, but not the topology. To get different topologies of embeddings, the free coordinates must be varied. The RCSR presently contains data for 1250 3-periodic structures with cubic symmetry. Of these, 141 have fixed coordinates and thus have a unique full symmetry embedding. These include basic nets like **srs**, the

Preprints (www.preprints.org) | NOT PEER-REVIEWED | Posted: 4 October 2023 doi:10.20944/preprints202310.0188.v1

unique 3-coordinated net with transitivity [1 1], the **dia** net of the diamond structure, and **pcu**, the net of the primitive cubic lattice. These, therefore, have a unique full symmetry embedding. But we showed earlier [1] that these all have topologically distinct lower symmetry embeddings.

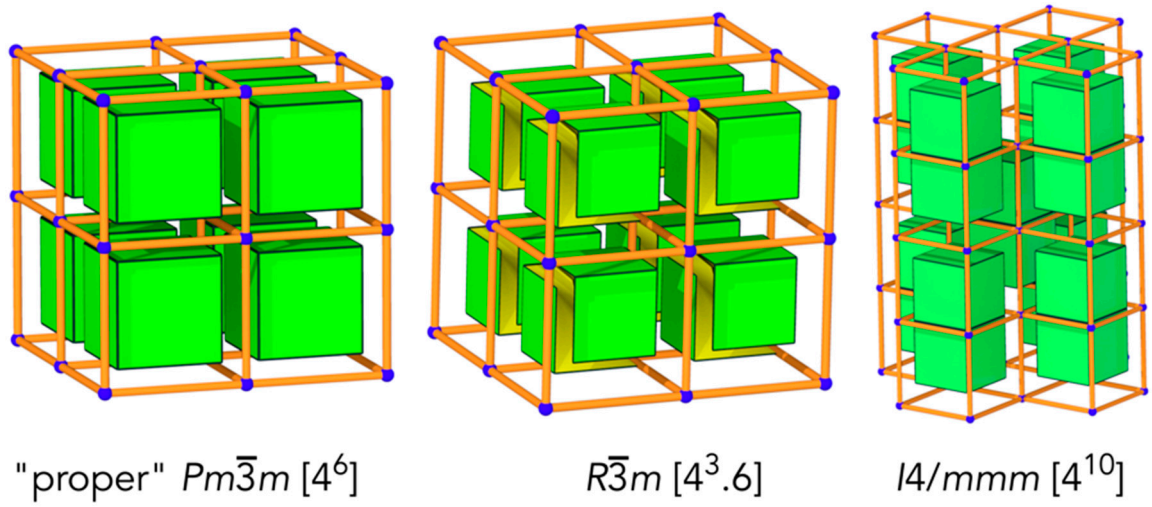

Figure 5. Examples of tilings of the **pcu** graph.

3.1. ana and rhr

Further examination of RCSR shows that, of the cubic graphs, 210 have just one free coordinate, and of these, just two, **ana** and **rhr**, have transitivity [1 1]. For **rhr**, the edge is specified as having symmetry $Im\bar{3}m$, with edges given by connecting vertices $x, x, 0$ to $1/2 - x, 1/2, 1/2 - x$, where x is the free parameter. Examination of girth for a wide range of x $(-3 \leq x \leq 3)$ shows that there is just one embedding (i.e., one ambient isotopy). This is readily shown to be tessellate, as illustrated in RCSR.

For **ana**, the edge is specified by space group $Ia\bar{3}d$, with edges between vertices $1/8, y, 1/4 - y$ to $y, 3/4 - y, -1/8$. Now, 32 embeddings are found for the free parameter y in the range $(-3 \leq y \leq 3)$. There is one large girth (1.0) embedding which admits a tiling. Two tiles are shown in Figure 6: an expanded trigonal prism $[6^2.8^3]$; the "two-headed fish" $[4^2.8^2]$, which is an expanded version of the 4-vertex trivalent graph shown. All the other embeddings are intricately tangled, have much lower girth (all with slender edges), and are decussate. We show in Figure 6 a fragment of the largest girth decussate structure (girth = 0.034); this has linked 4-rings inhibiting the formation of a tiling.

Preprints (www.preprints.org) | NOT PEER-REVIEWED | Posted: 4 October 2023 doi:10.20944/preprints202310.0188.v1

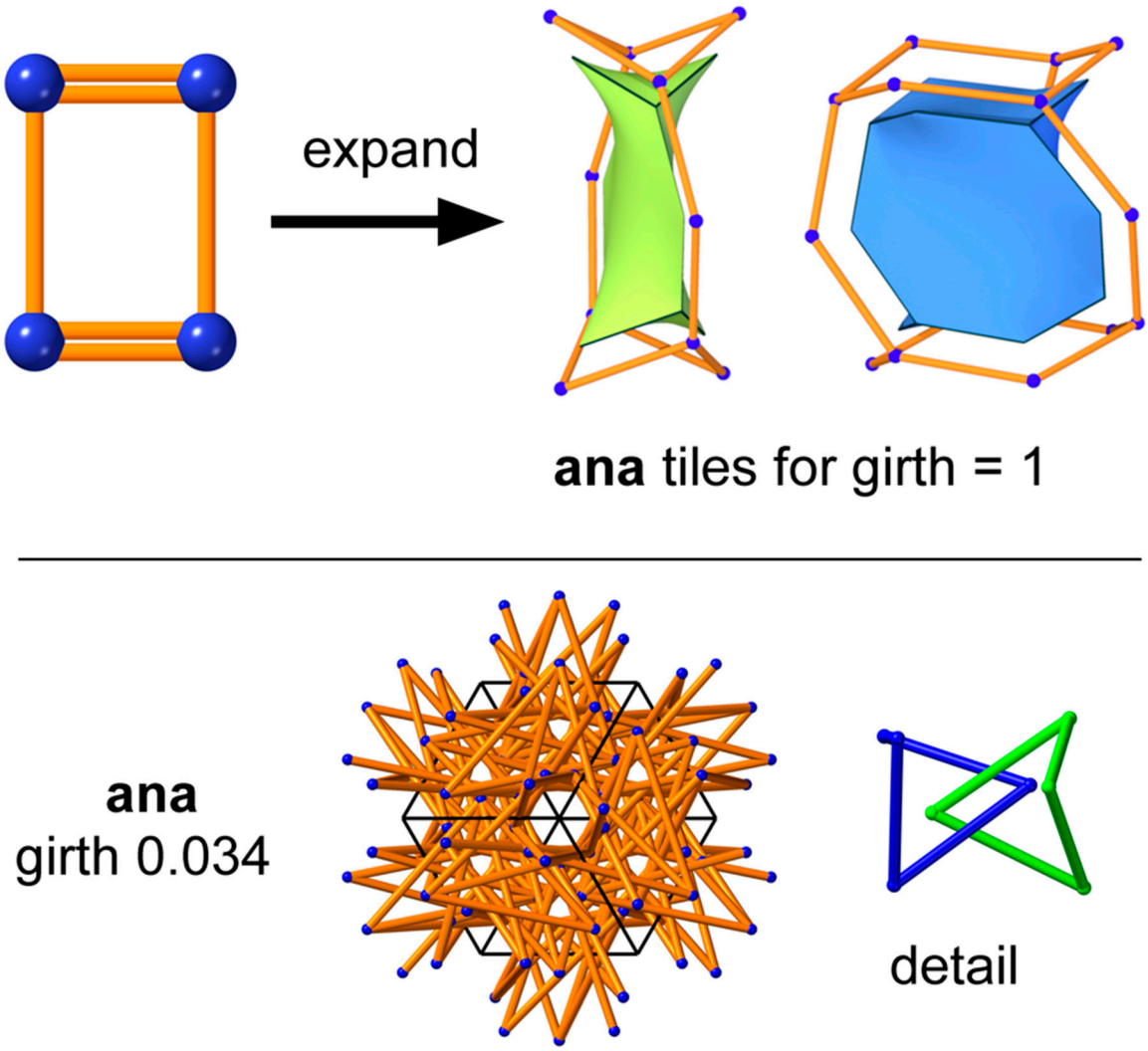

Figure 6. Top: $[4^2.8^2]$ and $[6^2.8^3]$ tiles of the tessellate embedding of the **ana** graph. Bottom: A fragment of the largest-girth decussate embedding of the **ana** graph; linked 4-rings are shown.

3.2. bmn

Turning to cubic graphs with one coordinate degree of freedom and transitivity [1 2] RCSR contains 42 entries. We examined just one in detail: **bmn**. This graph has symmetry $I4_132$, and edges are from $x, 0, 1/4$ to $1/4 - x, 0, 1/4$, and to $0, 1/4, 1/4 - x$. The largest-girth structure (girth = 1) is tessellate with a single space-filling cage [$6^2.14^3$], an extended trigonal prism. With x in the range $-3 \leq x < 3$ there are just three other embeddings. All three are clearly topologically distinct and decussate, as demonstrated in Figure 7. The largest girth (0.175) decussate structure has a knotted 6-ring (trefoil) and an unknotted 14-ring. In the second decussate structure, girth 0.082, neither ring is knotted, but the 14-rings are linked. In the third structure, girth 0.070, both the 6-ring and 14-ring are knotted and are also interlinked.

Preprints (www.preprints.org) | NOT PEER-REVIEWED | Posted: 4 October 2023 doi:10.20944/preprints202310.0188.v1

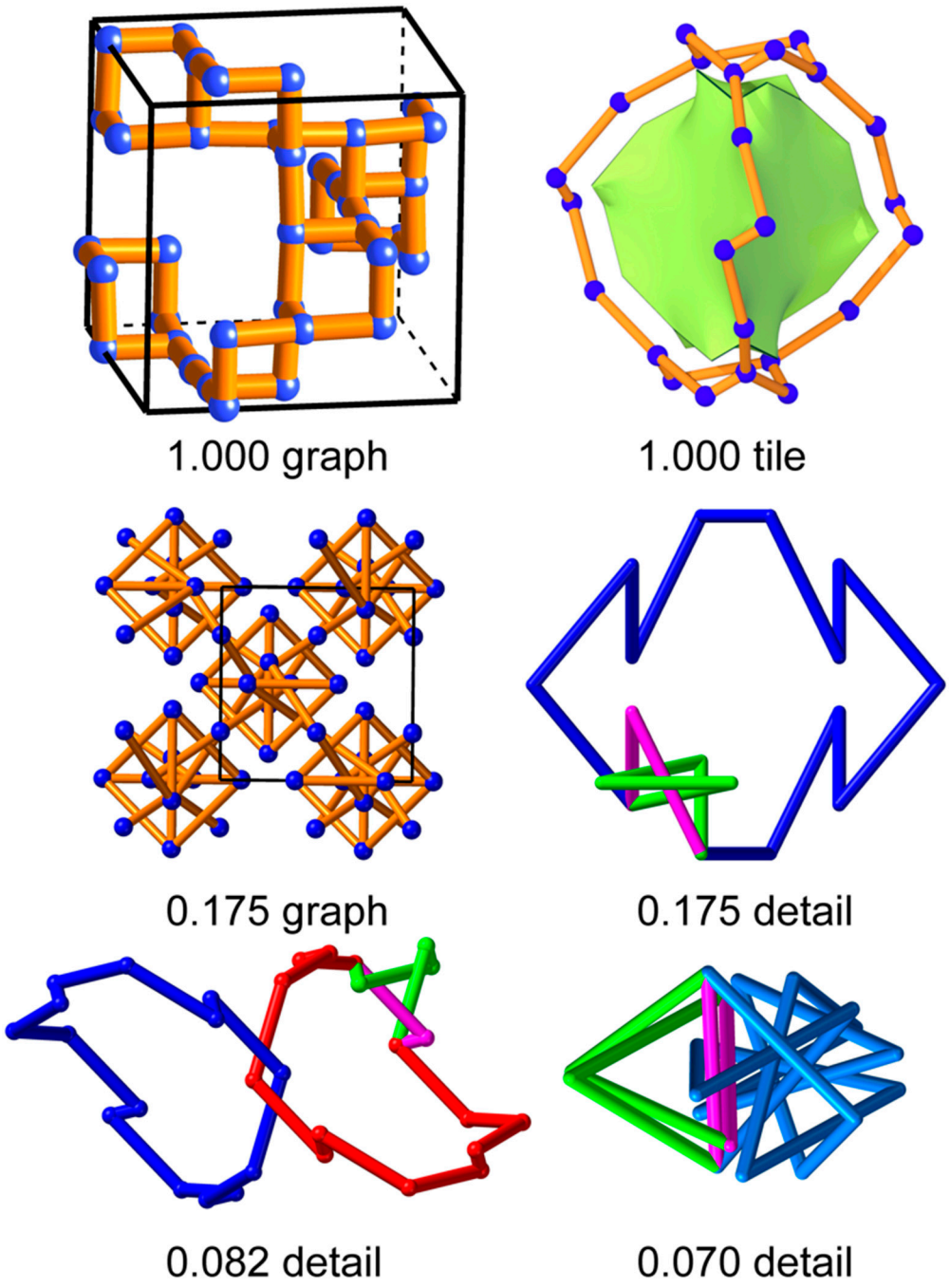

Figure 7. Four embeddings of the **bmn** graph, with girths of 1.0, 0.175, 0.082, and 0.070. Magenta edges are shared between 6-rings (green) and 14-rings (red and blue).

3.3. mok

The **mok** graph was originally introduced [10] as a simple example of a self-entangled periodic graph. As shown in Figure 8, it is composed of interlinked layers of interpenetrating honeycomb (**hcb**) graphs. It contains four cycles (strong rings) that are not the sum of smaller cycles, two 6-ring, an 8-ring, and a 10-ring. The 6-rings of the **hcb** layers are linked, but it transpires that a tiling can be constructed from the other three unlinked strong rings as shown in Figure 8. The transitivity is [1 3 3 2]. Thus, perhaps surprisingly, the existence of interlinking of the **hcb**-type layers does not proscribe a tessellate structure.

Preprints (www.preprints.org) | NOT PEER-REVIEWED | Posted: 4 October 2023 doi:10.20944/preprints202310.0188.v1

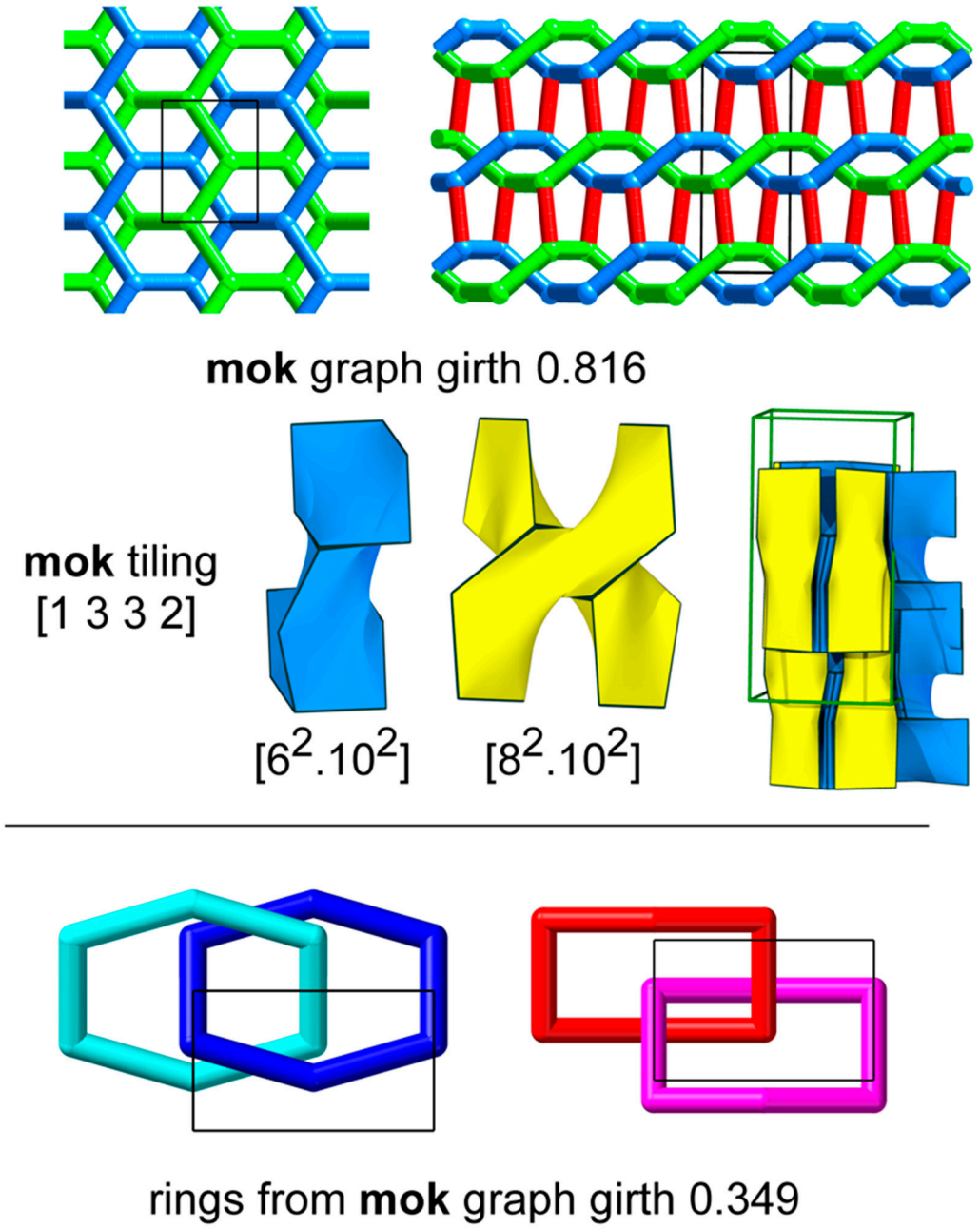

Figure 8. Top: an embedding of the **mok** graph with (on left), one layer. Middle: the two tiles that form a tiling of the **mok** graph. Bottom: showing the self-linking of the two types of 6-ring in a lower-girth embedding.

Vertex coordinates for the **mok** graph are of the form $x, y, 0$. The three symmetry-inequivalent edges are formed by connecting that vertex to its images at: $-x, -y, 0$; $1/2 - x, 1/2 - y, 0$; and $1 - x, y, -1/2$. For the free-parameter ranges $-1 \leq x,\ y < 1$, we find ten embeddings. The one tessellate embedding has the largest girth (0.816). The next-largest embedding, girth 0.349, is clearly decussate as both types of 6-rings are linked with other rings of the same kind, as shown in the figure.

3.4. jcy

A second graph was adduced [11] as being self-entangled, **jcy**. This graph, observed as the underlying graph of a crystal structure, has transitivity [3 3] and four coordinate degrees of freedom. The structure contains, as substructures, three sets of **hcb** nets interwoven, with an additional vertex linking triplets of **hcb** graphs. For a full symmetry ($P\bar{6}2c$) and vertex range ± 1, we find 34 embeddings of the underlying graph each with a different girth. We examined the two largest-girth

Preprints (www.preprints.org) | NOT PEER-REVIEWED | Posted: 4 October 2023 doi:10.20944/preprints202310.0188.v1

examples, shown in Figure 9. Both are clearly decussate, with linked 6-rings and linked 8-rings (these are the shortest cycles in the graph). As shown in the figure, the topological difference between the two embeddings is subtle, highlighting the need for a general method of distinguishing topologies. No tessellate embedding was found.

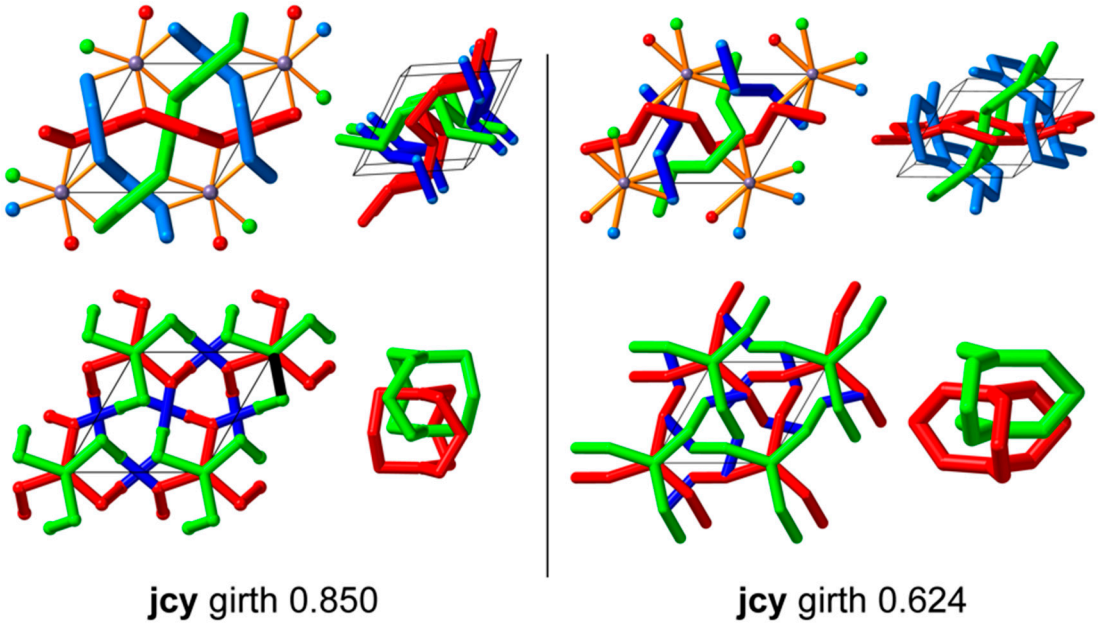

Figure 9. The two largest girth embeddings of the graph **jcy**. Top: showing the interlinking of honeycomb (**hcb**) nets, colored red, green, and blue. Below: showing the pattern of rods of [8_3] cages, colored red and green. Blue edges show the links between adjacent rods. In the larger-girth structure, the links (blue) between adjacent rods of 8-ring cages go outside the cages; In the smaller-girth structure, they go inside the cages.

3.5. fau

Zeolite structures are distinguished by a bold upper-case three-letter symbol such as **FAU** for the faujasite structure. These are recognized by the International Union of Pure and Applied Chemistry (IUPAC) to indicate "framework type" [12]. The simpler of these are in the RCSR with lower-case symbols, such as **fau**. **FAU** materials are of exceptional economic importance, so we have examined the full-symmetry ($Fd\bar{3}m$) embeddings of the **fau** graph, which has transitivity [1 4] and three variable coordinates. We find just three embeddings for a coordinate range of $-1 \leq x, y, z < 1$. As depicted in Figure 10, the girth = 1 structure is tessellate. This is the well-known structural form adopted by the alumino-silicate zeolite. The other two are distinct decussate embeddings. We can't resist adding that their girths are exactly $1/(\sqrt{2}+1)$ and $1/(\sqrt{6}+1)$.

Preprints (www.preprints.org) | NOT PEER-REVIEWED | Posted: 4 October 2023 doi:10.20944/preprints202310.0188.v1

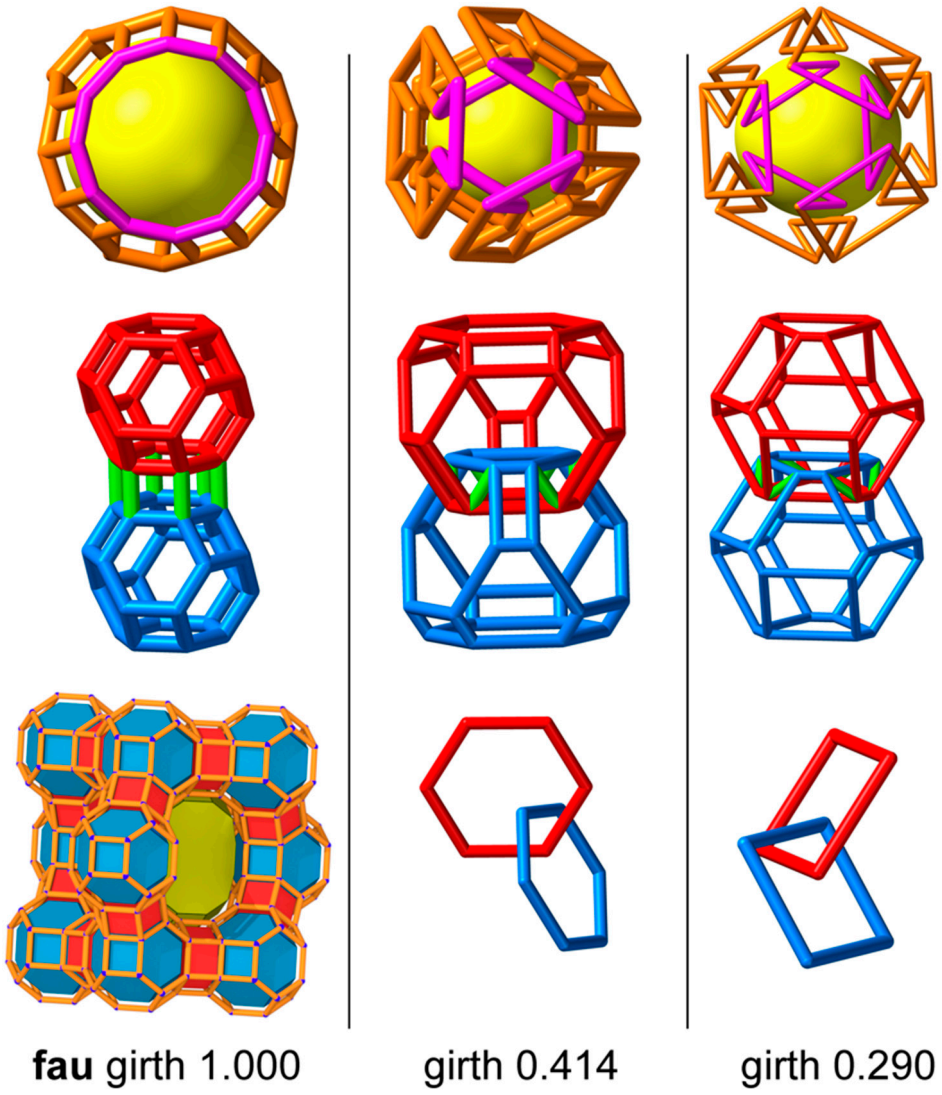

Figure 10. Embeddings of the **fau** graph. Top row: showing the conformation of the [$4^{18}.6^4.12^4$] cage. Second row: conformations of two connected sodalite cages ([$4^6.6^8$]) linked by a hexagonal prism. Bottom row left: the pattern of tiles in zeolite structure type **FAU**. Bottom, center and right: the linking of rings in the decussate structures.

4. Conclusions

We present some observations that we feel are relevant to the unanswered questions: (a) is there a preferred embedding of a graph that can unambiguously be called the "topology"?: and (b) how do we identify and distinguish between different embeddings (topologies) of a given graph?

For planar finite graphs, general usage is clear, and we take the unique tessellate embedding, particularly for polyhedra. All other embeddings are decussate as they contain knots and/or links and are referred to as tangles [13]. What is needed is a system of identifying each embedding in the same way as has been developed for knots and links. In this context, we remark that knots are just different embeddings of the graph of the unknot (a simple loop). There is an infinite number of knots, which by definition are decussate, but only one planar embedding – the unknot loop.

There may be tessellate embeddings for non-planar finite graphs, but as we have remarked for the case of K_{33}, an embedding with lower transitivity may be preferred as the default "topology".

Turning to periodic graphs: for a small number (some 3000) of particular interest in chemistry and materials science, an RCSR symbol leads to a specific embedding of that graph. But many more graphs have been identified. The *Topos* Topological Database has 200,000 "hypothetical and real nets

that have been observed" [14]. This suggests a pressing need for methods of distinguishing between various embeddings of these structures. As shown here, a periodic graph may have many embeddings, even at full symmetry.

The embeddings of graphs in RCSR, as reported by *Systre*, are obtained by finding the minimum density subject to the constraint of fixed equal-edge lengths. This approach was inspired by the observation [15] that such constrained maximum-volume configurations are often close approximations to the actual structure of simple ionic crystals. In our experience this is also the maximum-girth embedding, and, when it exists, the tessellate embedding.

An interesting open question is whether "there is at most only one tessellate embedding of a periodic graph?". We know of no counterexamples of graphs with two or more tessellate ambient isotopies. Further, our observations indicate that the tessellate embedding is always the maximum-girth embedding – it is the structure built with the stoutest sticks.

The use of the term *decussate* was inspired by Samuel Johnson's definition of "network" [16]: "Anything reticulated or decussated, at equal distances, with interstices between the intersections." This led, in turn, to the description of the science of linking together symmetric modules into (generally tessellate) periodic framework structures as *reticular chemistry* [17]. Recently, there has been a rapid increase in interest in synthesizing structures based on knots, periodic and finite links, tangles, weaving, knitting, and other decussate structures. The systematics of this might well be considered as *decussate chemistry*.

References

1. O'Keeffe, M. and M.M.J. Treacy, *The Symmetry and Topology of Finite and Periodic Graphs and Their Embeddings in Three-Dimensional Euclidean Space.* Symmetry, 2022. **14**: p. 822–841.
2. Earl, R. and J. Nicholson, *The Concise Oxford Dictionary of Mathematics*. 2021: Oxford University Press.
3. Blatov, V.A., A.P. Shevchenko, and D.M. Proserpio, *Applied Topological Analysis of Crystal Structures with the Program Package ToposPro.* Cryst. Growth Des., 2014. **14**(7): p. 3576–3586.
4. Delgado-Friedrichs, O. and M. O'Keeffe, *Identification of and symmetry computation for crystal nets.* Acta Crystallogr., 2003. **A59**: p. 351–360.
5. O'Keeffe, M., M.A. Peskov, S.J. Ramsden, and O.M. Yaghi, *The Reticular Chemistry Structure Resource (RCSR) database of, and symbols for, crystal nets.* Acc. Chem. Res., 2008. **41**: p. 1782–1789.
6. Blatov, V.A., O. Delgado-Friedrichs, M. O'Keeffe, and D.M. Proserpio, *Three-periodic nets and tilings: natural tilings for nets.* Acta Crystallogr., 2007. **A63**(5): p. 418–425.
7. Conway, J.H. and C.M. Gordon, *Knots and links in spatial graphs.* J. Graph Theory, 1983. **7**(4): p. 445–453.
8. O'Keeffe, M. and M.M.J. Treacy, *Tangled piecewise-linear embeddings of trivalent graphs.* Acta Crystallogr., 2022. **A78**: p. 128–138.
9. *Möbius Ladders and Related Molecular Graphs*, in *When Topology Meets Chemistry: A Topological Look at Molecular Chirality*, E. Flapan, Editor. 2000, Cambridge University Press: Cambridge. p. 69–109.
10. O'Keeffe, M., *Dense and rare four-connected nets.* Z. fur Krist. – Cryst. Mater., 1991. **196**(1–4): p. 21–38.
11. Bonneau, C. and M. O'Keeffe, *Intermetallic Crystal Structures as Foams. Beyond Frank–Kasper.* Inorg. Chem., 2015. **54**: p. 808–814.
12. Baerlocher, C., L.B. McCusker, and D.H. Olson, *Atlas of Zeolite Framework Types*. 6 ed. 2007 (http://www.iza-structure.org): Elsevier Science.
13. Hyde, S.T. and G.E. Schröder-Turk, *Tangled (up in) cubes.* Acta Crystallogr., 2007. **A63**: p. 186–197.
14. Alexandrov, E.V., A.P. Shevchenko, and V.A. Blatov, *Topological databases: why do we need them for design of coordination polymers?* Crystal Growth & Design, 2019. **19**(5): p. 2604–2614.
15. O'Keeffe, M., *On the arrangements of ions in crystals.* Acta Crystallogr., 1977. **A33**(6): p. 924–927.
16. Johnson, S., *Johnson's Dictionary Online* https://johnsonsdictionaryonline.com. 2023.
17. Yaghi, O.M., et al., *Reticular synthesis and the design of new materials.* Nature, 2003. **423**: p. 705–714.